

Article

Effect of Different Color Paste on Properties of Fluorine Resin/Aluminum Infrared Low Emissivity Coating

Xiaoxing Yan ^{1,2}

¹ Co-Innovation Center of Efficient Processing and Utilization of Forest Resources, Nanjing Forestry University, Nanjing 210037, China; xxyan255@126.com or yanxiaoxing@njfu.edu.cn

² College of Furnishings and Industrial Design, Nanjing Forestry University, Nanjing 210037, China

Received: 28 November 2019; Accepted: 8 January 2020; Published: 13 January 2020



Abstract: The effect of the four kinds of red, dark yellow, purple, and black pastes on the properties of fluorine resin/aluminum low emissivity coating was studied. The infrared emissivity coatings with red and black pastes were higher than the coatings with dark yellow and purple pastes. The hardness of the coatings with red, dark yellow, and purple color pastes was 6H, and that with black pastes was 6B. The adhesion and impact resistance of dark yellow coating was better, followed by red and purple, and the adhesion and impact resistance of black coating was the worst. Electrochemical polarization curves indicated that fluorine resin coatings with purple paste had better corrosion resistance. After the salt water resistance test, there was no obvious loss of light in the coatings with the four kinds of color pastes. The purple paste coating had no obvious loss of light and less bubble, suggesting that the fluorine resin/aluminum low emissivity coating with purple paste had better performance. The results of this study provide a new prospect for the application of infrared low emissivity coating in infrared stealth and compatibility with visible light.

Keywords: color paste; aluminum powder; fluorine resin; coating property

1. Introduction

At present, the research area related to infrared light is applied more and more in the military field. As a result, infrared low emissivity coating (IRLEC) has attracted more and more attention because infrared emissivity is an important index [1]. IRLEC is part of the infrared stealth technology [2]. Some universities, research institutes and so on have made relatively thorough research on IRLEC. Dong et al. [3] studied the reflection characteristics of infrared low emissivity camouflage coating in terahertz wave. Li et al. [4] prepared multilayer AlCrN/Cr/AlCrN coating on nickel matrix by cathodic arc ion plating, which is used in low infrared emissivity applications below 750 °C. Wang et al. [5] used polyethylene glycol (PEG) 400 and inorganic silicate binder to modify the CeO₂ filler with different content to prepare the coating with outstanding thermal shock resistance and low-temperature infrared emissivity. Corrosion is a problem because it limits the application of the coating. Corrosion protection is usually carried out by coating. The above researchers mainly focus on the reflection characteristics, thermal shock resistance and infrared emissivity, but less on the corrosion resistance, color [6] and compatibility with visible light. Infrared coating is required to have the following properties at the same time: low emissivity, environmental protection, good corrosion resistance, low gloss, so as to have a good effect on visible light compatibility. Fluorine resin is environmentally acceptable, not only has the high surface hardness, good adhesion, and corrosion resistance [7,8], but also can increase the water contact angle of the coating to achieve superhydrophobic properties [9–11].

Coating color is one of the important indicators of coating decoration performance, but different colors can resist different visible light detection [12]. For stealth coatings, besides low infrared emissivity,

it is also necessary to consider the compatibility with visible light stealth [13]. Therefore, it is necessary to reduce the brightness of the coatings and tone them [14]. Different color pastes can change the coating color of IRLEC; however, there are few relevant reports for IRLEC [15]. This paper mainly focused on the color matching problem, aiming to study the effect of quantitatively changing the dosage of different color pastes of red, dark yellow, purple, and black color pastes on the infrared emissivity, gloss, brightness, adhesion, impact resistance, corrosion resistance and roughness of fluorine resin/aluminum coatings, so as to obtain the optimum color of low gloss and IRLEC, laying a foundation for the application of IRLEC and compatibility with visible light in engineering.

2. Experimental Section

2.1. Experimental Materials

Fluorine resin (JF100) and curing agent: Juhua Group Co. Ltd., Quzhou, China. 4017 Al powder (M_w : 26.9815 g/mol, CAS No.: 7429-90-5, diameter: 10 μm , thickness: 220 nm, 65.0% Al powder mixed with 35.0% oleic acid): Zhangqiu Metal Pigment Co. Ltd., Zhangqiu, China. Red 8011 (solid concentration: 25.0%), dark yellow 8032 (solid concentration: 25.0%), purple 8005 (solid concentration: 15.0%), black 9927 (solid concentration: 20.0%): Suzhou Shiming Technology Co. Ltd., Suzhou, China. Technical aluminum plate [16]: 100 mm \times 50 mm \times 1 mm, Nanjing Chengxiang Aluminum Co. Ltd., Nanjing, China.

2.2. Preparation of Coating

Sandpapers were used to polish the pretreated substrate and to remove oil, and then they were dried in the oven. According to the previous research experience, the coating has good properties when the color paste content is 40% [17]. The solid content of aluminum powder and color pastes respectively referred to the quality of aluminum powder and color pastes respectively proportional to the quality of original aluminum powder and color pastes under the condition of vacuum (105 ± 2) $^\circ\text{C}$, where the aluminum powder and the color pastes were heated for 30 min. The solid content of fluorine resin and solid content of curing agent were measured according to the same method.

The coating was prepared according to the formula of Table 1. After mixing, the coating was coated on the surface of the flat technical aluminum plate. They were solidified at 40 $^\circ\text{C}$ for 2 h in a blast dryer. The thickness of the dry coating was about 60 μm .

Table 1. The composition of different color pastes.

Samples	Color Paste Coating				
	Red	Dark Yellow	Purple	Black	No Paste
Quality of fluorine resin (g)	3.0	3.0	3.0	3.0	3.0
Solid content of fluorine resin (%)	50.0	50.0	50.0	50.0	50.0
Quality of curing agent (g)	0.3	0.3	0.3	0.3	0.3
Solid content of curing agent (%)	90.0	90.0	90.0	90.0	90.0
Quality of aluminum powder (g)	1.815	1.815	1.815	1.815	1.815
Solid content of aluminum powder (%)	65.0	65.0	65.0	65.0	65.0
Quality of color paste (g)	2.83	2.83	4.72	3.54	0
Solid content of color paste (%)	25.0	25.0	15.0	20.0	0

Note: $\frac{\text{quality of aluminum powder} \times \text{solid content of aluminum powder}}{\text{quality of aluminum powder} + \text{quality of fluorine resin} + \text{quality of curing agent} + \text{solid content of curing agent}} \times 100\% = 40\%$
 $\frac{\text{quality of color paste} \times \text{solid content of color paste}}{\text{quality of fluorine resin} + \text{solid content of fluorine resin} + \text{quality of curing agent} + \text{solid content of fluorine resin}} \times 100\% = 40\%$

2.3. Test and Characterization

The specific information of the experimental test equipment is presented in Table 2. The infrared emissivity of the coating was tested in the range of 8–14 μm . In the test of corrosion resistance, a three-electrode battery structure was used for electrochemical tests. The saturated calomel electrode was used as the reference electrode and the platinum electrode as the counter electrode. The samples were immersed in 3.5% NaCl solution for 30 min and the open-circuit potential (OCP) was monitored

until constant. After the open-circuit potential was stabilized, the polarization tests were carried out. The test range was open-circuit potential ± 0.25 V. The coatings were immersed in 3.5% NaCl solution for 7 days, and the salt water resistance test was carried out. All the experiments were repeated four times with an error of less than 5.0%.

Table 2. Experimental test equipment.

Property	Standard	Equipment	Producer
thickness	-	JKTH-1250B digital coating thickness gauge	Tianjin Jingke Material Testing Machine Factory, Tianjin, China.
surface structure and morphology	-	JSM-5610LV scanning electron microscope	FEI Company in the United States, Hillsboro, USA.
infrared emissivity	-	Bruker Vertex 70 infrared emissivity tester	Chinese Academy of Sciences Shanghai Institute of Technological Physics, Shanghai, China.
gloss	GB/T 9754-2007	BGD512-60 vancometer	Shenzhen Sanenshi Technology Co. Ltd., Shenzhen, China.
impact resistance	GB/T 20624.2-2006	QCG paint film impact tester	Tianjin Precision Material Experiment Machine Factory, Tianjin, China.
adhesion	GB/T 4893.4-2013	QFH coating adhesion meter	Shenzhen Hanpu Testing Instrument Co. Ltd., Shenzhen, China.
hardness	GB/T 6739-2006	QHQ-A coating hardness meter	Quzhou Aipu Measuring Instrument Co. Ltd., Quzhou, China.
color difference	GB/T 3181-1995	SEGT-J colorimeter	Guangzhou Biaogeda Experimental Instruments Co. Ltd., Guangzhou, China.
roughness	GB/T 13288.5-2009	JB-4C precision roughness tester	Shanghai Taiming Optical Instrument Co. Ltd., Shanghai, China.
corrosion resistance	GB/T 15748-2013	CHI660E electrochemical workstation	Beijing Huakoputian Technology Co. Ltd., Beijing, China.
salt water resistance	GB/T 15748-2013	Beaker for 3.5% NaCl solution	Beijing Huakoputian Technology Co. Ltd., Beijing, China.

3. Results and discussion

3.1. Infrared Spectrum of Color Paste Corresponding to Coating

The infrared spectra of the four kinds of color paste corresponding to the coating are shown in Figure 1. The attribution of the peak is shown in Table 3. 3434 cm^{-1} had an obvious -OH absorption peak. 2943 cm^{-1} was -CH₃ absorption peak. 2874 cm^{-1} was -CH₂ absorption peak. 1750 cm^{-1} was -C=O- absorption [18,19]. 1441 cm^{-1} was the -COO absorption peak [20]. Obvious CF₃ absorption peak appeared at 1110 cm^{-1} [21].

IR absorption peaks indicated that fluorine resin formed covalent bond. According to Kirchhoff's law, in the state of heat balance, the infrared energy absorbed and emitted by an object is equal [22]. As can be seen in Figure 1, the infrared peaks of the purple coating, the dark yellow coating and the coating without paste were relatively flat, the infrared absorption was less, and the emittance of the corresponding coating was the lower (Figure 1), which was conducive to reduce the surface emissivity [23]. The black coating had more infrared absorption, so the surface emissivity was the highest, which was not conducive to the preparation of low infrared emissivity coating.

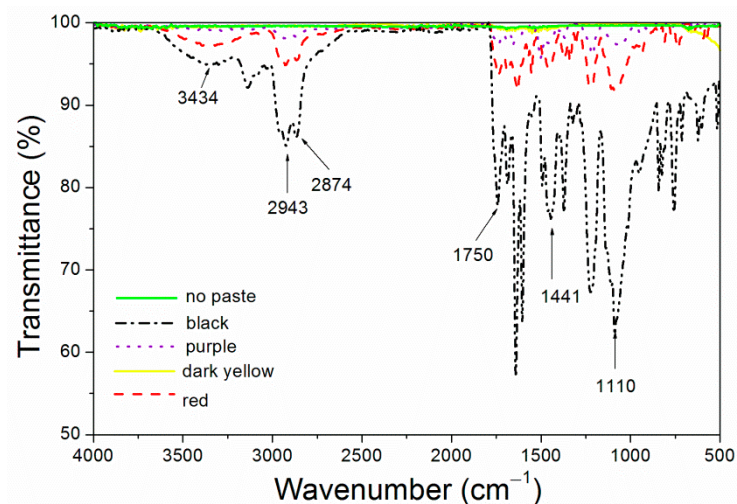


Figure 1. Infrared spectrum of the coatings with different color pastes.

Table 3. Assignment of peaks.

Peak (cm ⁻¹)	Assignment
3434	absorption of -OH
2943	absorption of -CH ₃
2874	absorption of -CH ₂
1750	absorption of -C=O-
1441	absorption of -COO
1110	absorption of -CF ₃

3.2. Influence of Color Paste on Infrared Emissivity of Coating

The influence of different color pastes on the infrared emissivity of fluorine resin coating is shown in Figure 2. The addition of red and black pastes made fluorine resin coating possess higher infrared emissivity (>0.3). Dark yellow and purple pastes could make fluorine resin coating possess lower infrared emissivity (0.10~0.25). Dark yellow paste had lower infrared emissivity than purple paste. This is due to the dark yellow paste had the lowest infrared absorption (Figure 1) and the strongest reflectivity compared with the other color pastes used in the experiment. The infrared emissivity of the dark yellow paste was the lowest [24].

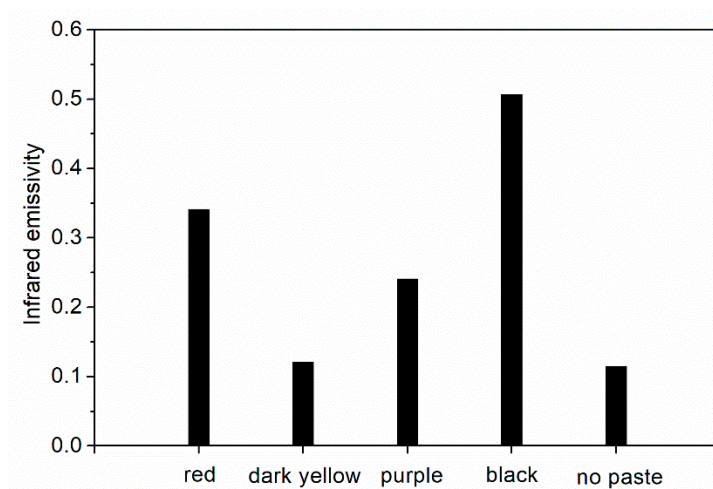


Figure 2. Influence of different color pastes on the infrared emissivity of the coating.

The SEM images of different color coatings are shown in Figure 3. There were more particles in red and black coatings, while obvious particles from microscopic view could hardly be noticed in dark yellow and purple pastes, and the coatings were more uniform, thereby reducing the absorption of infrared light and lowering the infrared emissivity [25]. More particles and voids increased the infrared absorption of coatings (Figure 1), so the infrared emissivity of red and black coatings increased.

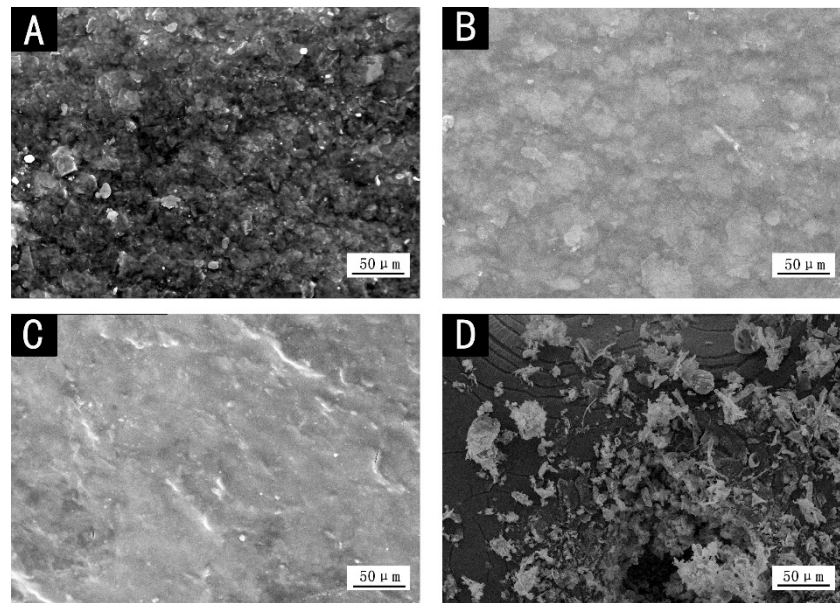


Figure 3. SEM images of different color coatings: (A) red, (B) dark yellow, (C) purple and (D) black.

3.3. Influence of Color Paste on Properties of Coatings

The effect of different color pastes on the properties of the coating is shown in Table 4. As shown in Table 4, compared with dark yellow and purple pastes, red and black pastes could make fluorine coatings possess lower luster. The gloss of black coating was the lowest. This is because the coatings with red and black pastes had a stronger ability to absorb and emit light and a weaker ability to reflect light, and therefore to present a lower gloss [26].

Table 4. Effect of color pastes on performance of the coatings.

Samples	Coatings				
	Red	Dark Yellow	Purple	Black	No Paste
Gloss (%)	11.4	12.4	17.5	4.3	23.0
Hardness	6H	6H	6H	6B	6H
Adhesion (level)	2	1	2	3	0
Impact resistance (kg·cm)	35	50	35	30	50
Roughness (μm)	1.29	0.947	0.625	5.214	0.500

Different color pastes have different effects on the hardness of coatings. The hardness of red, dark yellow, purple coating and the coating without paste was 6H, while the hardness of black coating was the lowest (6B). This is because black paste is mainly composed of carbon black particles. Compared with the other three pastes, carbon black particles are more loose affecting the compactness of the coating [27]. For low infrared emissivity coatings, an important role is to protect the covering, so the hardness cannot be too low [28]. It can be seen that the hardness of the coating added with black paste does not meet the basic hardness index (2H) [29]. For black coatings, in order to ensure that the coating can meet basic hardness index, the hardness can be enhanced by adding modifiers [30].

Table 4 indicated that the adhesion of the coating without paste was the best. The dark yellow coating had better adhesion and the black coating had the worst adhesion. This is because from a microscopic point of view, the dark yellow coating is more uniform and denser, and the components are easy to mix evenly, while the interaction between carbon black particles of black paste and other components of coating is less, so it is difficult to mix with them uniformly [31]. The influence of different color pastes on impact resistance of the coating was different. The black coating had the lowest impact resistance, while the dark yellow coating and the coating without paste had the highest. This is because the dark yellow coating and the coating without paste has high adhesion. Good adhesion can ensure good impact resistance. The adhesion of coatings with black pastes is relatively small, and it is easy to fall off when impacted [32].

As can be seen in Table 4, the roughness of dark yellow and purple coatings was lower, and the surface was smoother. The roughness of black coatings was the highest. This may be because the smaller particle size of the dark yellow and purple pastes, which can fill the gap between the aluminum powder in the coating and increase the compactness of the coating. The carbon black particles of the black paste aggregate together to form large particles, thus increasing the roughness [33].

Table 5 is the effect of four kinds of color pastes on the chromatic aberration of coatings. The color difference refers to the difference of the overall brightness and hue of the coating [34]. L , a and b represent the brightness, red-green and yellow-blue value of different color coating respectively. L' , a' and b' represent these values of the substrate itself. The difference ΔL , Δa and Δb are obtained by subtracting them, which are respectively expressed as lightness difference, red-green index difference and yellow-blue index difference. Thus, the color difference ΔE can be obtained according to the formula [35].

Table 5. Effect of color pastes on ΔE of the coatings.

Sample	Coatings				
	Red	Dark Yellow	Purple	Black	No Paste
L	53.8	65.2	30.9	71.6	67.8
a	28.7	7.8	22.1	5.4	1.1
b	4.6	35.2	−32.2	−1.7	−2.3
L'	25.9	25.9	25.9	25.9	25.9
a'	5.2	5.2	5.2	5.2	5.2
b'	−3.1	−3.1	−3.1	−3.1	−3.1
ΔL	27.9	39.3	5.0	45.7	41.9
Δa	23.5	2.6	16.9	0.2	−4.1
Δb	7.7	38.3	−29.1	1.4	0.8
ΔE	37.3	54.9	34.0	45.7	42.1

According to Table 5, the effect of different color pastes on color difference of the coatings was different. The color difference of purple paste was the smallest compared with that of red, dark yellow and black pastes. At the same time, the L value of purple coating was the lowest, which made the coating darker. The other three coatings had larger L value and were brighter.

From the above study, it can be found that the coatings with purple, red, and dark yellow pastes have better comprehensive performance. Therefore, the electrochemical corrosion resistance of these three coatings was tested. The test results are shown in Figure 4 and Table 6. The β_a and β_c are respectively the anode Tafel slope and the cathode Tafel slope [36]. The unit is mv/dec, mv refers to the voltage, and dec refers to the logarithmic current. The higher the potential E_{corr} , the greater the resistance R_p , and the smaller the current I_{corr} and the better the corrosion resistance.

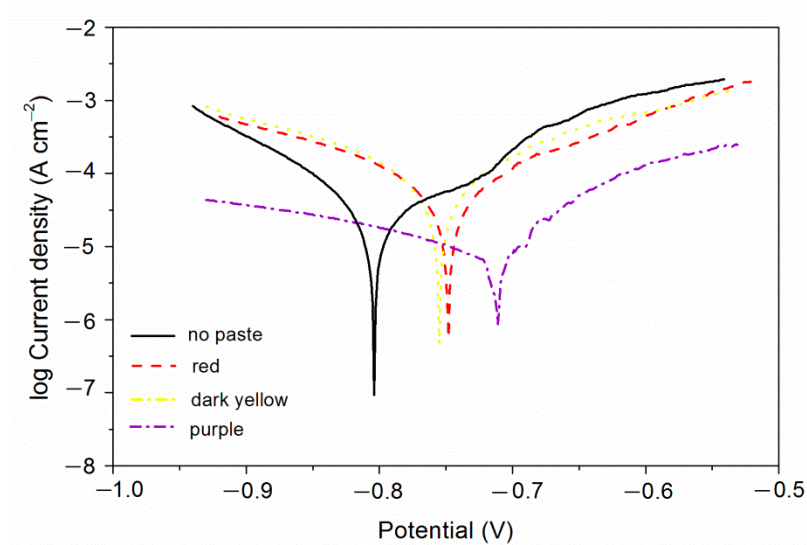


Figure 4. Electrochemistry diagram of different color pastes.

Table 6. Effect of different color pastes content on corrosion resistance.

Sample	Coatings			
	Red	Dark Yellow	Purple	No Paste
E_{corr} (V)	−0.75	−0.76	−0.71	−0.80
R_p (Ω/cm^2)	415.5	343.1	1301.1	670.2
I_{corr} (A/cm^2)	8.78×10^{-5}	1.00×10^{-4}	2.76×10^{-5}	2.79×10^{-5}
β_a (mV/dec)	163	144	124	73
β_c (mV/dec)	172	175	248	105

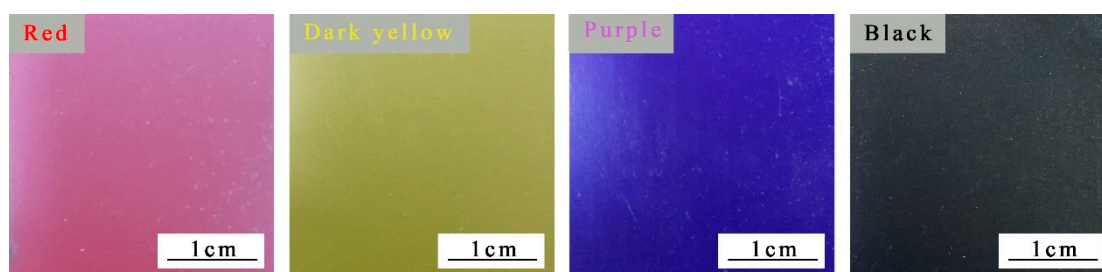
The salt water resistance of coatings with four color pastes immersed in 3.5% NaCl solution for 7 days was tested to observe the change of surface condition after a certain corrosion time. The loss of light, discoloration, and foaming density in the actual corrosion process of the paint film were evaluated. When the loss of light was <3%, 4–15%, 16–30%, 31–50%, 51–80% and >80%, respectively, the degree of loss of light of coatings were at the 0, 1, 2, 3, 4, and 5 level, respectively. When the change of color difference before and after salt water resistance was <1.5, 1.6–3.0, 3.1–6.0, 6.1–9.0, 9.1–12.0 and >12.0, respectively, the degree of loss of light of coatings was non-discoloration, very slight discoloration, slight discoloration, obvious discoloration, severe discoloration and complete discoloration, and the grades were 0, 1, 2, 3, 4 and 5 level, respectively. The test results are shown in Tables 7 and 8, and Figure 5.

Table 7. Change of loss of light.

Sample	Coatings				
	Red	Dark Yellow	Purple	Black	No Paste
Gloss before immersion (%)	11.4	12.4	17.5	4.3	23.0
Gloss after immersion (%)	11.4	12.0	13.0	2.0	21.7
Loss of light (%)	0	0.4	4.5	2.3	1.3
Grade of loss of light (level)	0	0	1	0	0

Table 8. Color difference change after salt solution test.

Sample	Coatings				
	Red	Dark Yellow	Purple	Black	No Paste
<i>L</i>	55.2	68.3	34.5	30.0	74.5
<i>a</i>	34.3	5.2	17.4	3.3	1.4
<i>b</i>	5.3	44.0	−32.4	4.4	−2.2
<i>L'</i>	25.9	25.9	25.9	25.9	25.9
<i>a'</i>	5.2	5.2	5.2	5.2	5.2
<i>b'</i>	−3.1	−3.1	−3.1	−3.1	−3.1
ΔL	29.3	42.4	8.6	4.1	48.6
Δa	29.1	0	12.2	−1.9	−3.8
Δb	8.4	47.1	−29.3	7.5	0.9
ΔE	42.1	63.4	32.9	8.8	48.8
Chromatic aberration before and after salt water resistance	4.8	8.5	1.1	36.9	6.7
Color change grade (level)	2	3	0	5	3

**Figure 5.** Foaming profile of fluorine resin coating for red, dark yellow, purple and black pastes.

As can be seen in Table 7, the coatings had no obvious loss of light. The loss of light grade was 0 or 1, indicating that fluorine resin coatings with different color pastes had good corrosion resistance. As can be seen in Table 8, there was no obvious discoloration of the purple coating. The discoloration grade was 0, indicating that the purple coating had better corrosion resistance, which was consistent with the results of electrochemical testing (Figure 4). Under the same experimental conditions, the dark yellow coating and the black coating changed color obviously, and the color change grade was at level 3 or above.

As can be seen in Figure 5, the coating was destroyed after 7 days of 3.5% NaCl solution immersion for the corrosion resistance test, and coatings with color pastes had a certain degree of foaming. The foaming density of dark yellow and purple coatings was lower, and black coating had a small amount of foaming, while red foaming was more serious. The compact coating and little pores (Figure 3B,C) can prevent the NaCl solution from entering, improve the corrosion resistance of the coating, and not easily cause the phenomenon of light loss, discoloration, and bubbling.

Based on the above analysis, it can be concluded that purple 8005 can be used to prepare low infrared emissivity fluorine resin coatings with better performance. The structure of purple 8005 paste was characterized. SEM image of purple 8005 is shown in Figure 6, and the infrared spectrum is shown in Figure 7.

Figure 6 showed that the size of purple 8005 paste was small. As can be seen in Figure 7, purple 8005 paste contains abundant organic functional groups [37]. 3314 cm^{-1} , 2963 cm^{-1} , 1638 cm^{-1} and 1560 cm^{-1} corresponded to the characteristic absorption peaks of N-H, C-H, C=C and C-N respectively, so they were easy to disperse in fluorine resin coatings and had good compatibility with fluorine resin coatings.

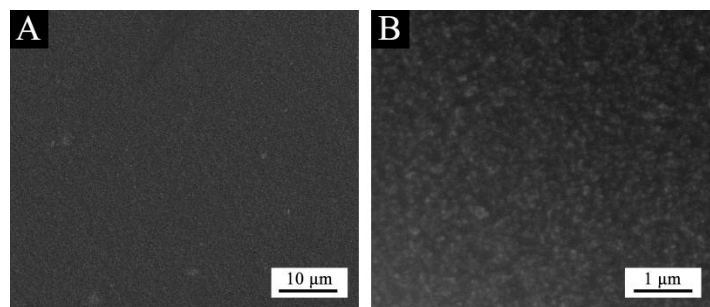


Figure 6. SEM image of purple paste: (A) low and (B) high magnification.

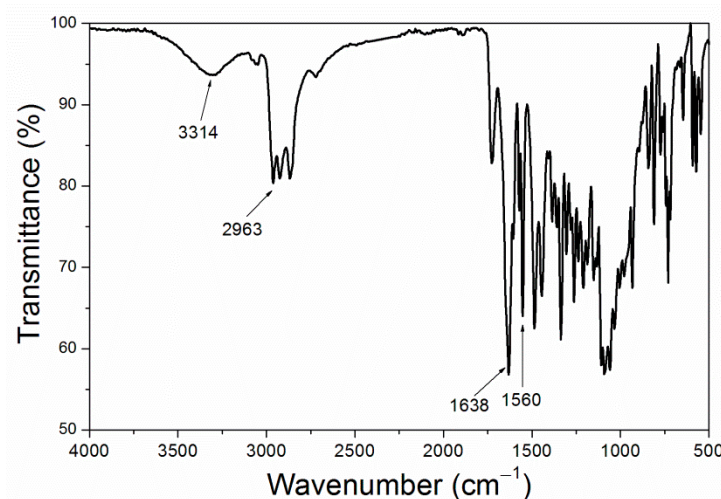


Figure 7. Infrared spectrum of purple paste.

4. Conclusions

The four kinds of red, dark yellow, purple, and black color pastes were added into the fluorine resin coating system, so that the fluorine resin coating has low infrared emissivity, low gloss, low brightness, good adhesion, and impact resistance, as well as low roughness. Purple paste can make fluorine resin coating possess low infrared emissivity and better comprehensive properties. The salt water resistance test showed that the coatings with red, dark yellow, purple, and black color pastes had no obvious loss of light. The purple coating had no obvious discoloration, and the dark yellow and black coatings had obvious discoloration under the same experimental conditions. The foaming densities of the dark yellow and purple coatings were less, i.e., the fluorine resin coating with the purple paste has the better performance. This work provides a new prospect for the compatibility with visible light stealth of low infrared emissive coatings in engineering.

Funding: This research received no external funding.

Acknowledgments: This project is supported by the Youth Science and Technology Innovation Fund of Nanjing Forestry University (CX2016018).

Conflicts of Interest: The authors declare no conflict of interest.

References

1. Liang, J.; Li, W.; Xu, G.Y.; Meng, X.; Liu, K.; Tan, S.J. Preparation and characterization of the colored coating with low infrared emissivity based on nanometer pigment. *Prog. Org. Coat.* **2018**, *115*, 74–78. [[CrossRef](#)]
2. Fang, K.Y.; Fang, F. Au-decorated SWNT/PVDF electrospun films with enhanced infrared stealth performance. *Mater. Lett.* **2018**, *230*, 279–282. [[CrossRef](#)]
3. Dong, H.L.; Wang, J.C.; Zeng, Y.R.; Chen, Z.S.; Shi, J.M. Reflection spectrum study of THz wave by infrared low emissivity stealth coating. *Spectrosc. Spect. Anal.* **2019**, *39*, 3007–3012.

4. Li, Q.Y.; Dong, S.J.; Cao, Q.; Ye, W.P.; Gong, D.Q.; Cheng, X.D. Thermal stability of multi-layered AlCrN/Cr/AlCrN coatings at elevated temperatures for low thermal emissivity applications. *Appl. Surf. Sci.* **2019**, *498*, 143886. [[CrossRef](#)]
5. Wang, L.; Xu, G.Y.; Liu, C.Y.; Hou, H.L.; Tan, S.J. Surface-modified CeO₂ coating with excellent thermal shock resistance performance and low infrared emissivity at high-temperature. *Surf. Coat. Technol.* **2019**, *357*, 559–566. [[CrossRef](#)]
6. Liu, Y.; Hu, J.; Wu, Z.H. Fabrication of coatings with structural color on a wood surface. *Coatings* **2020**, *10*, 32. [[CrossRef](#)]
7. Chen, T.; Peng, C.H.; Liu, C.; Yuan, C.H.; Hong, J.; Chen, G.R.; Xu, Y.T.; Dai, L.Z. Modification of epoxy resin with a phosphorus, nitrogen, and fluorine containing polymer to improve the flame retardant and hydrophobic properties. *Macromol. Mater. Eng.* **2019**, *304*, 1800498. [[CrossRef](#)]
8. Yan, X.X. Effect of black paste on the property of fluorine resin/aluminum infrared coating. *Coatings* **2019**, *9*, 597. [[CrossRef](#)]
9. Cakmakci, E. HDI trimer based fluorine containing urethane methacrylates for hydrophobic photocured coatings. *Polym. Plast. Technol. Mater.* **2019**, *58*, 854–865. [[CrossRef](#)]
10. Zhang, J.; Lin, W.Q.; Zhu, C.X.; Lv, J.; Zhang, W.C.; Feng, J. Dark, infrared reflective, and superhydrophobic coatings by waterborne resins. *Langmuir* **2018**, *34*, 5600–5605. [[CrossRef](#)] [[PubMed](#)]
11. Rodic, P.; Milosev, I. One-step ultrasound fabrication of corrosion resistant, self-cleaning and anti-icing coatings on aluminium. *Surf. Coat. Technol.* **2019**, *369*, 175–185. [[CrossRef](#)]
12. Peng, L.H.; Jiang, S.X.; Guo, R.H.; Xu, J.T.; Li, X.T.; Miao, D.G.; Wang, Y.X.; Shang, S.M. IR protection property and color performance of TiO₂/Cu/TiO₂ coated polyester fabrics. *J. Mater. Sci. Mater. Electron.* **2018**, *29*, 16188–16198. [[CrossRef](#)]
13. Wang, K.Z.; Wang, C.X.; Yin, Y.J.; Chen, K.L. Modification of Al pigment with graphene for infrared/visual stealth compatible fabric coating. *J. Alloys Compd.* **2017**, *690*, 741–748. [[CrossRef](#)]
14. Bekhta, P.; Krystofiak, T.; Proszkyk, S.; Lis, B. Surface gloss of lacquered medium density fibreboard panels veneered with thermally compressed birch wood. *Prog. Org. Coat.* **2018**, *117*, 10–19. [[CrossRef](#)]
15. Kolanowska, A.; Kuziel, A.W.; Herman, A.P.; Jedrysiak, R.G.; Gizewski, T.; Boncel, S. Electroconductive textile coatings from pastes based on individualized multi-wall carbon nanotubes—Synergy of surfactant and nanotube aspect ratio. *Prog. Org. Coat.* **2019**, *130*, 260–269. [[CrossRef](#)]
16. Rodic, P.; Milosev, I. Corrosion inhibition of pure aluminium and alloys AA2024-T3 and AA7075-T6 by cerium(III) and cerium(IV) salts. *J. Electrochem. Soc.* **2016**, *163*, C85–C93. [[CrossRef](#)]
17. He, L.H.; Zhao, Y.; Xing, L.Y.; Liu, P.G.; Zhang, Y.W.; Wang, Z.Y. Low infrared emissivity coating based on graphene surface-modified flaky aluminum. *Materials* **2018**, *11*, 1502. [[CrossRef](#)]
18. Maiti, K.S. Ultrafast N-H vibrational dynamics of hydrogen-bonded cyclic amide reveal by 2DIR spectroscopy. *Chem. Phys.* **2018**, *515*, 509–512. [[CrossRef](#)]
19. Sun, S.J.; Zhao, Z.Y.; Umemura, K. Further exploration of sucrose-citric acid adhesive: Synthesis and application on plywood. *Polymers* **2019**, *11*, 1875. [[CrossRef](#)]
20. Palencia, M. Functional transformation of fourier-transform mid-infrared spectrum for improving spectral specificity by simple algorithm based on wavelet-like functions. *J. Adv. Res.* **2018**, *14*, 53–62. [[CrossRef](#)]
21. Holtomo, O.; Motapon, O.; Nsangou, M. DFT study of photochemical properties and radiative forcing efficiency features of the stereoisomers cis- and trans-CHCl=CH-CF₃. *J. Phys. Chem. A* **2019**, *123*, 10437–10445. [[CrossRef](#)] [[PubMed](#)]
22. Guevelou, S.; Rousseau, B.; Domingues, G.; Vicente, J. A simple expression for the normal spectral emittance of open-cell foams composed of optically thick and smooth struts. *J. Quant. Spectrosc. Radiat. Transf.* **2017**, *189*, 329–338. [[CrossRef](#)]
23. Echaniz, T.; Perez-Saez, R.B.; Tello, M.J. Optical properties of metals: Infrared emissivity in the anomalous skin effect spectral region. *J. Appl. Phys.* **2014**, *116*, 093508. [[CrossRef](#)]
24. Wackelgard, E.; Svedung, H. Optical characterization and modelling of paint top-coatings for low-emittance applications. *Infrared Phys. Technol.* **2016**, *78*, 275–281. [[CrossRef](#)]
25. Canagaratna, M.R.; Massoli, P.; Browne, E.C.; Franklin, J.P.; Wilson, K.R.; Onasch, T.B.; Kirchstetter, T.W.; Fortner, E.C.; Kolb, C.E.; Jayne, J.T.; et al. Chemical compositions of black carbon particle cores and coatings via soot particle aerosol mass spectrometry with photoionization and electron ionization. *J. Phys. Chem. A* **2015**, *119*, 4589–4599. [[CrossRef](#)] [[PubMed](#)]

26. England, G.T.; Russell, C.; Shirman, E.; Kay, T.; Vogel, N.; Aizenberg, J. The optical janus effect: Asymmetric structural color reflection materials. *Adv. Mater.* **2017**, *29*, 1606876. [[CrossRef](#)]
27. Souri, H.; Bhattacharyya, D. Highly sensitive, stretchable and wearable strain sensors using fragmented conductive cotton fabric. *J. Mater. Chem. C* **2018**, *6*, 10524–10531. [[CrossRef](#)]
28. Koshuro, V.A.; Fomin, A.A.; Rodionov, I.V.; Fomina, M.A. The effect of microarc oxidation on the structure and hardness of aluminum-oxide coatings formed by plasma spraying on titanium. *Prot. Met. Phys. Chem. Surf.* **2018**, *54*, 840–844. [[CrossRef](#)]
29. Nikfar, Z.; Shariatnia, Z. Phosphate functionalized (4,4)-armchair CNTs as novel drug delivery systems for alendronate and etidronate anti-osteoporosis drugs. *J. Mol. Graph. Model.* **2017**, *76*, 86–105. [[CrossRef](#)]
30. Bhogayata, A.C.; Arora, N.K. Workability, strength, and durability of concrete containing recycled plastic fibers and styrene-butadiene rubber latex. *Constr. Build. Mater.* **2018**, *180*, 382–395. [[CrossRef](#)]
31. Kao, C.Y.; Chou, K.S. Iron/carbon-black composite nanoparticles as an iron electrode material in a paste type rechargeable alkaline battery. *J. Powder Sources* **2010**, *195*, 2399–2404. [[CrossRef](#)]
32. Nguyen, C.L.; Preston, A.; Tran, A.T.T.; Dickinson, M.; Metson, J.B. Adhesion enhancement of titanium nitride coating on aluminum casting alloy by intrinsic microstructures. *Appl. Surf. Sci.* **2016**, *377*, 174–179. [[CrossRef](#)]
33. Kim, W.; Bae, J.; Eum, C.H.; Jung, J.; Lee, S. Study on dispersibility of thermally stable carbon black particles in ink using asymmetric flow field-flow fractionation (AsFFFF). *Microchem. J.* **2018**, *142*, 167–174. [[CrossRef](#)]
34. Gomez, O.; Perales, E.; Chorro, E.; Burgos, F.J.; Viqueira, V.; Vilaseca, M.; Martinez-Verdu, F.M.; Pujol, J. Visual and instrumental assessments of color differences in automotive coatings. *Color Res. Appl.* **2016**, *41*, 384–391. [[CrossRef](#)]
35. Medina, J.M.; Diaz, J.A. Fluctuation scaling of color variability in automotive metallic add-on parts. *Prog. Org. Coat.* **2017**, *104*, 118–124. [[CrossRef](#)]
36. Sykes, J.M.; Xu, Y. Electrochemical studies of galvanic action beneath organic coatings. *Prog. Org. Coat.* **2012**, *74*, 320–325. [[CrossRef](#)]
37. Fuertes, N.; Bengtsson, V.; Pettersson, R.; Rohwerder, M. Use of SVET to evaluate corrosion resistance of heat tinted stainless steel welds and effect of post-weld cleaning. *Mater. Corros.* **2017**, *68*, 7–19. [[CrossRef](#)]



© 2020 by the author. Licensee MDPI, Basel, Switzerland. This article is an open access article distributed under the terms and conditions of the Creative Commons Attribution (CC BY) license (<http://creativecommons.org/licenses/by/4.0/>).